Estuarine, Coastal and Shelf Science 223 (2019) 39–49

Contents lists available at ScienceDirect

Estuarine, Coastal and Shelf Science

journal homepage: www.elsevier.com/locate/ecss

Climate change during the Little Ice Age from the Lake Hamana sediment record

Ara Cho[a], Kaoru Kashima[a], Koji Seto[b], Kazuyoshi Yamada[c], Takumi Sato[b,d], Kota Katsuki[b,*]

[a] Department of Earth and Planetary Sciences, Faculty of Sciences, Kyushu University, Fukuoka, 819-0395, Japan
[b] Estuary Research Center, Shimane University, Matsue, 690-8504, Japan
[c] Museum of Natural and Environmental History, Shizuoka, Shizuoka, 422-8017, Japan
[d] Interdisciplinary Faculty of Science and Engineering, Shimane University, Matsue, 690-8504, Japan

ARTICLE INFO

Keywords:
Diatom
Chemical components
Lagoon
Typhoon
Monsoon
Paleoenvironment

ABSTRACT

Paleoenvironment and paleoclimate changes during the Little Ice Age (LIA) were investigated using sediments from Lake Hamana. This lagoon in central Japan is under a complicated climate system influenced by the East Asian summer monsoon (EASM), East Asian winter monsoon (EAWM), and strong typhoon events. Diatom assemblages and chemical components of a 1.3 m sediment core suggest historical events of rapid salination and cyclical ecosystem shifts accompanied by monsoon condition changes. Most research has indicated that Lake Hamana changed from a freshwater lake to a brackish lagoon because of the Meio earthquake in 1498 CE. However, based on results from the diatom assemblage and chemical components, this salination occurred because of changes in the Hamana paleoriver flow, and this change happened before the earthquake, around the mid-15th century. Furthermore, it is clear that Lake Hamana was an oligohaline lagoon before salination. The lithology of the lake sediments and the diatom assemblage changed during the LIA; sand, water, and total diatom contents decreased. However, the relative abundance of marine diatom taxa increased during the LIA. These changes were introduced by a weakening EASM coupled with low precipitation under low solar activity during the LIA. Several flood events represented by freshwater diatom taxa and magnetic susceptibility peaks co-occurred with strong El Niño events during the LIA. It is inferred that this strong El Niño during the LIA induced frequent typhoons causing floods in central Japan.

1. Introduction

Japan has a complicated climate system influenced by the East Asian summer monsoon (EASM), East Asian winter monsoon (EAWM), and strong typhoon events. In summer, climate in central and southern Japan is controlled by the Pacific High, which leads to high rainfall and small seasonal temperature variations. In contrast, the continental Siberian High brings dry and large seasonal temperature variations in winter. Both the EASM and EAWM have anticorrelated effects on lake sediments, and the balance of the monsoon forcing is dependent on the location of the intertropical convergence zone (ITCZ) (Yancheva et al., 2007). Japan is also moderately affected by typhoons, which have generated heavy rainfall events averaging three times per year for the past ten years (Japan Meteorological Agency, 2018). From June to October, typhoons crossed Shizuoka prefecture, in central Japan, once or twice per year for the last five years (Fig. 1) (Japan Meteorological Agency, 2018).

Paleoclimate change research in lagoonal systems can be difficult because lagoons are easily affected by sea level change. Recently, however, many studies reconstructing paleoclimate based on microfossils have been performed in lagoonal systems because they provide valuable information on environmental changes at a variety of temporal and spatial scales (Woodward et al., 2014; Peros et al., 2015). Furthermore, ample evidence for ancient typhoons has been obtained by chemical analysis of lagoon sediments (Woodruff et al., 2009, 2015; Katsuki et al., 2016, 2017). Paleoenvironmental change research has been performed on sediments from Lake Hamana examining its salinity and ecology change (Kashima, 1988; Morita et al., 1998; Sato et al., 2016). In addition historical documents state that the inlet of Lake Hamana was modified by a large earthquake (Yata, 2005). A detailed record of environmental change in recent centuries is still unclear due to poor age control of the Lake Hamana sediment deposits, and the record of the impact of the Meio earthquake in 1498 CE is also unclear. Climate change research in Lake Hamana is also rare for the same

* Corresponding author.
E-mail address: kkota@soc.shimane-u.ac.jp (K. Katsuki).

https://doi.org/10.1016/j.ecss.2019.04.033
Received 22 August 2018; Received in revised form 10 April 2019; Accepted 17 April 2019
Available online 22 April 2019
0272-7714/ © 2019 Elsevier Ltd. All rights reserved.

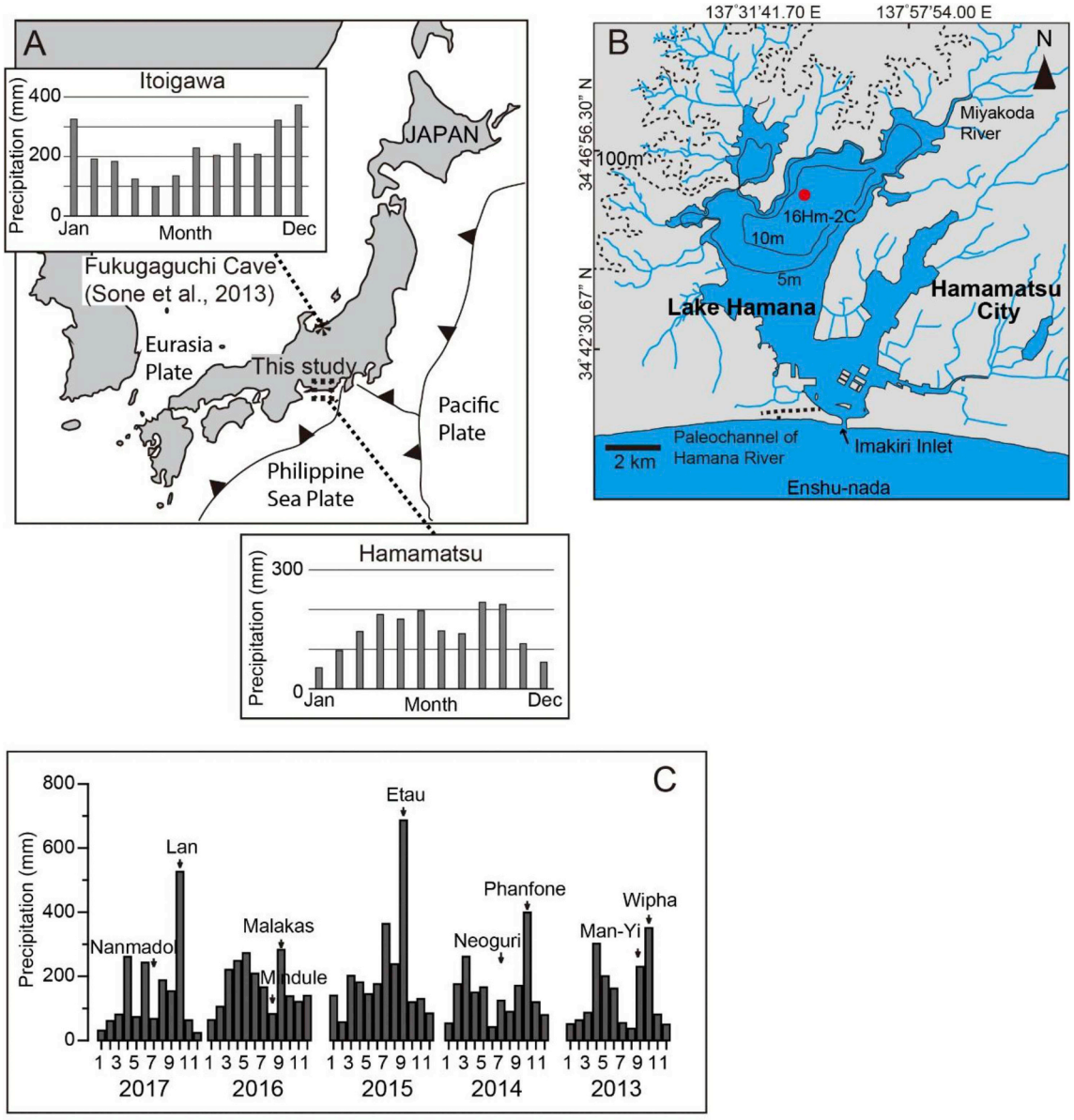

Fig. 1. Location of the study area and monthly average precipitation: (A) map of Japan and study site location. Monthly average precipitation of Hamamatsu and Itoigawa from 2008 to 2017. (B) Core site (16Hm-2C) at Lake Hamana. (C) Hamamatsu monthly average precipitation from 2013 to 2017, showing heavy rainfall due to typhoons (Lan, Malakas, Etau, Phanfone, Man-Yi, and Wipha).

reason.

Diatoms are microalgal paleoenvironmental indicators and vital primary producers capable of photosynthesis in all waters where sunlight is available. They are very sensitive to environmental change, such as variation in water temperature, pH, and nutrients. Climate can control catchment processes, which affect nutrients, pH, and temperature (Anderson, 2000). Thus, changes to any one of these ecological factors significantly impact the biological form, growth, colony formation, and geographical distribution of diatom assemblages. The diatoms leave their valves in the sediment, and diatoms preserve a record of climate change. Therefore, diatoms are useful for reconstruction of paleoenvironmental and climate changes (Kashima, 1985, 1986; Ryu et al., 2003). In this work, we examine how the EASM and EAWM modify the climate in both eastern Japan and western Japan inferred from chemical components, diatom assemblage and diatom abundance in Lake Hamana sediments, which are controlled by precipitation and nutrients. Furthermore, flood layers, which were observed in the sediment cores and recorded in historical documents suggest a relationship between typhoons and El Niño/Southern Oscillation (ENSO) during the Little Ice Age (LIA).

2. Study area

Lake Hamana, located in Shizuoka Prefecture in central Japan, is a coastal lagoon with a surface area of approximately 65 km^2 and an average depth of 4.8 m (Fig. 1). The average water depth of the northern part of Lake Hamana is 10–12 m and 2–3 m in the southern region (Sato et al., 2016). Lake Hamana contains brackish water today because the lake is connected to the Pacific Ocean. The average tidal range in 2017 was 240 cm, and high tide and low tide were 360 and 145 cm respectively (Japan Meteorological Agency, 2017). There is a gradient in surface salinity across the lake; salinity was 19–21 psμ near inflowing streams, and salinity increased up to 29 psμ near the coast in the summer season. The salinity of the bottom water is 29 psμ (Taguchi and Nakata, 1998).

Lake Hamana is surrounded by mountains, hills, and terraces. Three

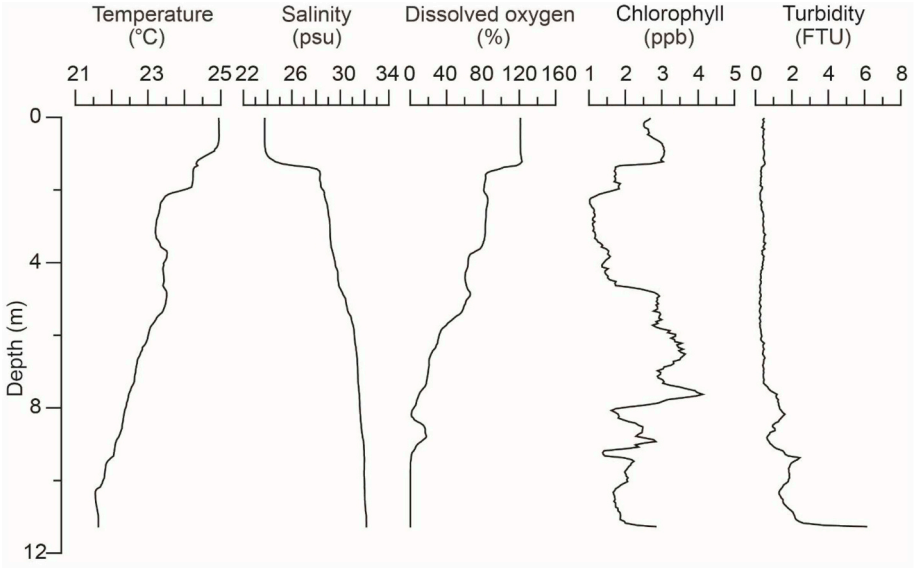

Fig. 2. Variations in temperature, salinity, dissolved oxygen, chlorophyll and turbidity against water depth at the coring site, June 2016.

terraces, the Tenpakubara, Kamoe, and Mikatagahara terraces, were developed during the middle to late Pleistocene, and are distributed along its eastern and western shores (Isomi and Inoue, 1972; Muto, 1987; Sugiyama, 1991; Nakashima et al., 2008). Six coastal sand barriers are located along the Enshu-nada coast (Matsubara, 2001, 2007) (Fig. 1).

2.1. Tectonic movement

The Nankai Trough is located close to the Enshu-nada coastal plain. Along the Nakai Trough, the Phillippine Sea plate moves beneath the Eurasian plate (Fig. 1). This Nankai Trough is the locus of recent earthquakes associated with tsunami (Fujiwara et al., 2013). According to historical documents, large earthquakes which generated severe damage have occurred along the Nankai Trough (Yata, 2009). It is reported that the lake has been a brackish lagoon since the Meio

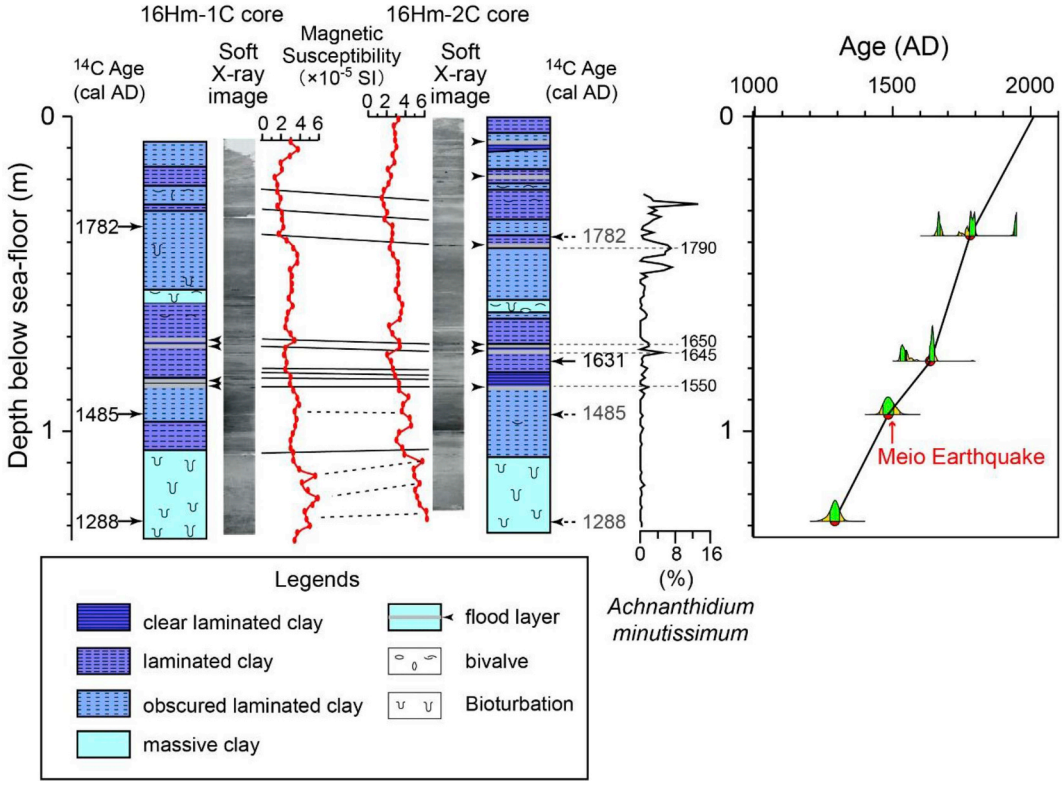

Fig. 3. Lithology description, soft X-ray image, magnetic susceptibility, and age-depth plot for cores 16Hm-1C and 16Hm-2C. Yellow and green ranges in age-depth plot are the age range of 1 and 2 sigma, relatively. The abundance of *Achnanthidium minutissimum* in 16Hm-2C is also shown. The obscured lamina can hardly be seen with the naked eye, however indistinct layers can be confirmed in soft-X ray image. (For interpretation of the references to color in this figure legend, the reader is referred to the Web version of this article.)

earthquake in 1498, when the sand dune barrier was broken and a marine inlet opened (Fujiwara et al., 2006, 2013). Tsunami deposits caused by Meio earthquake have been found in the nearby coastal plain, although not in the lake sediments.

3. Materials and methods

Water quality at the coring site was measured when the cores were taken (Fig. 2). Measurements of water depth, water temperature, salinity, chlorophyll, and turbidity were taken at 1-s intervals with an AAQ-RINKO system (Alec Electronics, Japan). The depth precision of the AAQ-RINKO is 0.3%. The 16Hm-1C and 16Hm-2C cores were obtained from the northern part of Lake Hamana (E137°34.995′, N34°45.912') at a water depth of 11.56 m on 30th June 2016 using a pneumatic piston corer and hand push piston corer, respectively (Fig. 1). The 16Hm-2C core was collected because the upper part of the 16Hm-1C core was lost; the 16Hm-1C core was used only for core chronology. The 1.3 m long core 16Hm-2C is 6.2 cm in diameter. Diatom assemblage, chemical components, magnetic susceptibility, sand content, and water content in the 16Hm-2C core were analyzed from 25 cm to 130 cm at a 1 cm interval. A soft X-ray image was taken using a 25 cm length case. To analyze the water content, the weight of each sample was compared before and after freeze drying. A portion of the dried samples were sieved at 63-μm mesh. After picking out the calcareous material from the sieved samples, the weight of the remaining coarse sample was used to calculate sand content.

3.1. Chronology of core 16Hm-2C

The age model was constructed by ^{14}C dating obtained from two cores: 16Hm-1C and 2C, both from the same location. The lithology of the two sediment cores was compared and correlated using physical properties, such as density and magnetic susceptibility (Fig. 3). The ^{14}C ages of two plant fragments, one shell, and one possible seagrass samples were measured using accelerator mass spectrometry (AMS) dating (Linick et al., 1989) (Table 1). These samples were washed repeatedly using an ultrasonic cleaner, and then chemically cleaned using acid-alkali-acid treatments to remove secondary contamination. Samples of radiocarbon-free wood were treated using the same procedure to serve as blanks. These samples and standard samples (NIST OxII, IAEA C-7, and IAEA C-8) were combusted using an elemental analyzer. CO_2 gases were purified cryogenically in a high-vacuum automatic preparation system and then converted to graphite via reduction on Fe-powder with hydrogen gas in a quartz tube. The ^{14}C ages of the samples were measured at the AMS facility in Paleo Labo Co., Ltd in Gunma Prefecture of Japan. Carbon isotopic fractionations were corrected using $\delta^{13}C$ values measured at the AMS facility. The ^{14}C ages were calculated and converted to calendar dates using IntCal13 (Reimer et al., 2013) and CALIB 7.1 (Stuiver and Reimer, 1993). The two samples at 95 and 129 cm depths were calibrated by the marine 13 data-set and the local marine reservoir effect should be considered. However, the ΔR values have not yet been documented in Lake Hamana. The lake is located on the Pacific Side of central Japan and the Kuroshio current flows near the inlet of Lake Hamana. ΔR values in regions belonging to the Kuroshio Current system have been reported: 73 ± 17 years in Taiwan, 29 ± 18 years in the Ryukyu Islands, and −22 ± 18 years in the Ogasawara Islands (Yoneda et al., 2007). Also, ΔR values reported from the Miura Peninsula were 82 ± 33 yr and 77 ± 32 yr (Shishikura et al., 2007). The range of ΔR value might be from −22 to 82 years. However, ΔR values in brackish lakes are generally smaller than coastal marine regions because of the freshwater input. Therefore, here, we estimate the ΔR value at close to zero in the 16Hm-1C and 16Hm-2C cores.

3.2. Chemical component analysis

Samples of the 16Hm-2C core were prepared by freeze-drying and grinding. After drying, 1N HCl solution was added to a 10 mg sample in a silver container to remove inorganic carbon and then heated on a hot plate for 4 h. Dried samples were then loaded into tin capsules. Total organic carbon (TOC), total nitrogen (TN), and total sulfur (TS) were determined by a CHNS material analyzer, Thermo ELECTRON CORPORATION, model Flash EA 1112. The ratios of C/N and C/S were calculated from the TOC, TN, and TS values. The accuracy of the procedure was controlled by standard BBOT (2,5-Bis-(5-tert.-butyl-benzoxazole-2-yl)-thiophene), which was measured after every ten sediment samples.

3.3. Diatom analysis

Diatom assemblages were analyzed from 25 cm to 130 cm in the 16Hm-2C core at 1 cm intervals, using 0.01 g of dry sediment. Dry sediments were placed into a 200 ml beaker with 10 ml of 30% H_2O_2 to eliminate organic matter. After boiling for 1 h, 200 ml of distilled water was added to each beaker and samples were soaked for 4 h. Water was decanted and replaced twice with new distilled water, and additional distilled water was added three times to separate higher density substances from diatoms. The remaining bottom solutions of 0.2–0.8 ml after decantation were pipetted onto a coverslip using a micropipette and mounted with Pleurax. At least 300 diatom valves were counted on each slide under 2000 × magnification by light microscope. Diatoms were classified based on classification schemes used in previous studies (Hendey, 1964; Round et al., 1990; Takano, 1990; Kojima et al., 1995; Hasle and Syvertsen, 1996; Watanabe, 2005; Kobayashi et al., 2006).

Table 1
Radiocarbon age data from core 16Hm-1C and 16Hm-2C, Lake Hamana. Radiocarbon dates were calculated and converted to calendar dates with IntCal13 (Reimer et al., 2013) and CALIB 7.0 (Stuiver and Reimer, 1993).

Depth below sea floor (cm)	C^{13}/C^{12} Ratio (‰)	Conventional		Calibrated C^{14} Age 1 sigma (Cal AD)					Lab.No.	Sample No.	Material
		C^{14} Age (yr BP)	std. (yr)			Median Probability	Range	Probablity			
38.3	−30.83	202	17	intcal13	AD	1782	(1662–1673) (1778–1799) (1942–1950)[a]	0.239 0.548 0.213	PLD-33242	16Hm-1C-27	plant
78	−30.31	279	19	intcal13	AD	1631	(1528–1544) (1549–1550) (1634–1652)	0.351 0.033 0.616	PLD-35544	16Hm-2C-78	plant
95	−0.32	821	17	marine13	AD	1485	(1465–1504)	1.000	PLD-33240	16Hm-1C-86.5	shell
129	−11.77	1104	19	marine13	AD	1288	(1273–1308)	1.000	PLD-35545	16Hm-1C-120.5	seagrass?

[a] This standard deviation (error) includes a lab error multiplier.

The following equation calculated the total diatom valves and Diatom Accumulation rate (DAR):

Total diatom valves per 1 g dry sediment [No. g^{-1}] = Counted valves on slide [No.] × Observation area (slide area [mm^{-2}]/counted area [mm^{-2}]) × Liquid volume used (beaker liquid volume [ml])/micropipette volume [μL]) × 1000 × $sediment^{-1}$ [g^{-1}].

Diatom Accumulation Rate (DAR) [No. valves cm^{-2} kyr^{-1}] = (No. valves g^{-1} dry sediment) [No. g^{-1}] × (dry bulk density) [g cm^{-3}] × (sedimentation rate) [cm kyr^{-1}].

4. Results

4.1. Water stratification at the coring site

Vertical water quality measurements at the coring site were carried out just before obtaining the sediment cores. The surface temperature on 30 June 2016 was 25 °C and 21 °C at the bottom of Lake Hamana (Fig. 2). The salinity was around 24 psμ; however, it suddenly increased to 34 psμ below a depth of 1.8 m (Fig. 2). Similarly, chlorophyll and dissolved oxygen (DO) dropped drastically at the 1.8 m depth, with chlorophyll increasing again between 4.2 and 7.7 m. Turbidity was low down to 8 m and increased strongly up to 7 (FTU) at 11.9 m.

4.2. 16Hm-2C core

The sediment of the 16Hm-2C core was dominated by laminated clay with disarticulated bivalves to the 109 cm depth, while bioturbation was observed below 109 cm (Fig. 3). High-density layers including sand were deposited at 40.5, 72.0, 74.0, and 87.0 cm depths (Fig. 3). To avoid core top disturbance, we began our study at a depth of 25-cm. High-density layers represented by dark colors on the soft X-ray image appear several times (Fig. 3). The range of magnetic susceptibility is from 1 to 6 × 10^{-5} SI (Fig. 3). TOC, C/N and C/S ratios are 1.5–4.5 (%), 8.8 to 11.2 and 0.4 to 2.4, respectively (Fig. 4). Sand and water

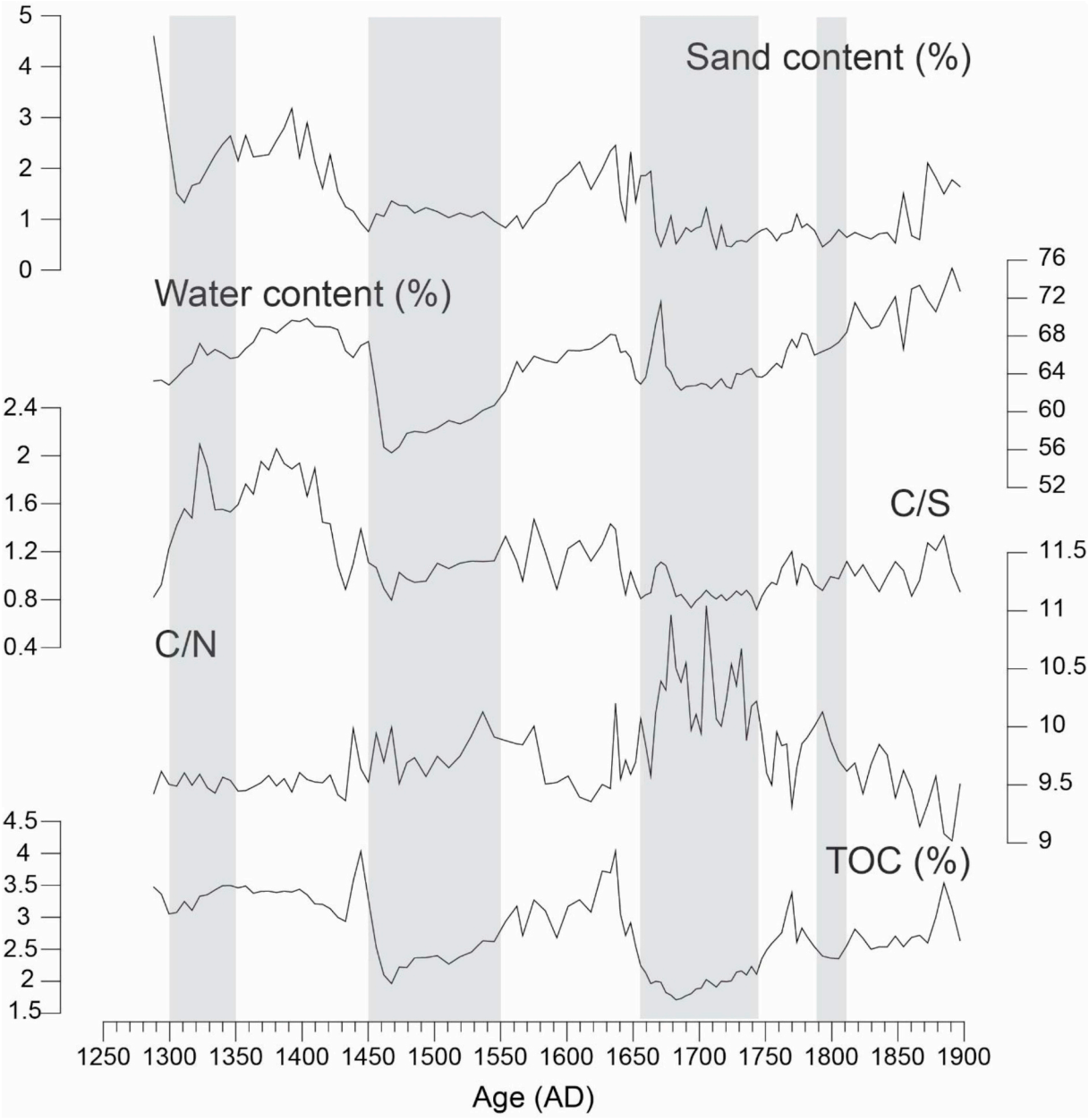

Fig. 4. Sand content, water content, C/S, C/N ratio and TOC in core 16Hm-2C. Gray zones represent intervals of climate change based on the chemical components and diatom assemblage.

Table 2
Diatom ecology in 16Hm -2C, Lake Hamana.

Genus species	Ecology		Inhabitat	Reference
Aulacoseira ambigua	Generally mesotrophic to eutrophication	Freshwater	River and lake	Joh, 2010
Aulacoseira granulata	Mesotrophic to eutrophication	Freshwater	Rive and stream	Joh, 2010
Cyclotella atomus	Eutrophic and halotolerant diatom	Freshwater to brackish	River and lake	Joh, 2010
Cyclotella atomus var. *gracilis*	Prefer euryhaline and eutrophic condition	Freshwater to brackish		Genkal and Kiss, 1993
Cocconeis scutellum	Benthic on aquatic plant	Brackish to marine	Coastal area and lagoon	Joh, 2012
Diploneis smithii		Brackish to marine	Coastal area	Hendy, 1964
Fallacia nyella		Marine	Tropical coast	Witkowski et al., 2000
Podosira stelligera		Marine	Sea and coastal area	Hendy, 1964
Pseudostaurosira brevistriata	Oligotrophic condition	Freshwater	Lake	Joh, 2012
Thalassiosira lineata		Marine	Sea	Park et al., 2016
Thalassiosira nano-lineata		Marine	Sea	Park et al., 2016
Thalassionema nitzschioides		Marine	Neritic zone	Hallegraeff, 1986

content showed similar tendencies and fluctuated from 0.5 to 4.6% and from 55.7 to 75.2%, respectively (Fig. 4).

Twelve diatom taxa were dominant in the 16Hm-2C core (Table 2). The taxa reaching more than 10% relative abundance were *Aulacoseira ambigua*, *Aulacoseira granulata, Pseudostaurosira brevistriata, Cyclotella atomus, Cyclotella atomus* var. *gracilis, Cocconeis scutellum, Thalassionema nitzschioides*, and *Thalassiosira lineata* (Fig. 5). The taxa with relative abundances below 10% were *Diploneis smithii, Fallacia nyella*, *Podosira stelligera*, and *Thalassiosira nano-lineata. Aulacoseira ambigua* and *A. granulata* dominated, and *P. brevistriata* start increasing before 1440 CE. After 1440 CE, *C. atomus, C. atomus* var. *gracilis, C. scutellum, D. smithii, F. nyella, P. stelligera, T. nitzschioides*, *T. lineata,* and *T. nano-lineata* showed high percentages. The abundance of *Achnanthidium minutissimum* has several peaks (Fig. 3). The total diatom valve indicates the number of valves in 1 g dry sample and diatom accumulation rate (DAR) is the annual diatom accumulation. These two graphs have a very similar pattern (Fig. 5).

5. Discussion

5.1. Environmental changes before and after the Meio earthquake 1498 CE

The Meio earthquake in 1498 CE generated a tsunami that is documented in the written record (Watanabe, 1998). Previous studies suggested that the Imakari inlet (Fig. 1) between Lake Hamana and the North Pacific Ocean was formed and that the opening of this inlet led to the lake transitioning from freshwater to brackish lagoon following the Meio earthquake. One study indicates that Lake Hamana was previously connected to the Pacific Ocean via the Hamana river, a short tributary that was lost after the earthquake (Fujiwara et al., 2013). Tsunami deposits have been identified as thick sand beds on the floodplain of the Hamana River (Fujiwara et al., 2013). However, in the lake a dramatic change of the diatom assemblage probably occurred in the mid-15th century, well before the Meio earthquake (Fig. 5). Marine diatoms appeared, and *A. ambigua* and *A. granulata*, which are freshwater species (Joh, 2010), suddenly disappeared at 1440 CE in the 16Hm-2C core (Fig. 5). The lithology also changed from clay with bioturbation to laminated clay and the halophilic species *C. atomus* increased significantly (Joh, 2010) around the 109 cm depth, at approximately 1400 CE, in the 16Hm1C and 16Hm2C cores (Figs. 3 and 5). *Aulacoseira granulata* prefers conditions of vertically active water and is vulnerable to standing water (Joh, 2010). These results imply that there was active lake water circulation before the 15 t h century, leading to high DO in the bottom layer of Lake Hamana, shown by the core's bioturbated sediment. Based on historical documents, the Hamana River connected an enclosed embayment (the present-day Lake Hamana) to the Pacific Ocean during the 14 and 15th centuries (Ebara, 2008; Yata, 2009). In addition, geological data supports a Hamana paleoriver channel that flowed to the Pacific until at least 1340–1400 CE (Fujiwara et al., 2013). In the southwestern floodplain next to Lake Hamana, an estuarine environment was terminated by the development of coastal sand dunes and beach-ridge plains in the 13–15th centuries, and a brackish-freshwater marsh environment was present in this area (Fujiwara et al., 2006, 2013). Freshwater diatom taxa were dominant in Lake Hamana before the mid-15th century represented by this floodplain development, suggesting that seawater inflow was prevented by the expanded coastal beach. However, the diatom assemblage data from the 16Hm-2C core suggests that seawater exchange with the Pacific Ocean through the Hamana paleoriver increased at about the mid 15th century, well before the Meio earthquake. Furthermore, the brackish-freshwater species, *Cyclotella atomus* started to increase around 1415 CE (Fig. 5). After the Meio earthquake, the Hamana paleoriver was lost, and the present inlet was created. The water exchange rate with the Pacific Ocean throughout this new inlet was higher than the exchange in the mid-15 century. Note that some uncertainty remains in the core chronology, although the delta-R values are most likely close to zero, if an uncertainty of ± 30 years is incorporated into the calibrated marine 14C dates in the core, a very small chance exists that the diatom transition level (1.06 m) dates to ~1500 and the Meio earthquake. We should emphasize, however, that this is unlikely.

Some previous reports have suggested that Lake Hamana was a freshwater lake before the Meio earthquake (Morita et al., 1998; Sato et al., 2016). Although freshwater diatom taxa are dominant before the Meio earthquake, the lake was not completely freshwater based on the C/S ratio. The range in C/S ratio is 0.7–2.1 through the 16Hm-2C core. Prior to 1440 CE, the C/S ratio increased to 2 (Fig. 4). This value strongly suggests that the lake was affected by marine water (Berner and Raiswell, 1984). This difference between the diatom assemblage and C/S ratio indicates that Lake Hamana had seasonal stratification before the earthquake. The salinity of the bottom water was higher than surface water due to the inflow of seawater through the sand bar of the Hamana paleoriver. Therefore, the lake was not a freshwater lake but was an oligohaline lake before the Meio earthquake.

5.2. Climate change related to EASM and EAWM

As mentioned above, seasonal change in Japan is tied to the EASM and EAWM. In East Asia, monsoonal climate variability occurs in centennial to millennial-scale cycles since the late Holocene (Gupta et al., 2003), which are primarily related to solar radiation (Gupta et al., 2003; Wang et al., 2005). Previous studies agree that the EASM is anticorrelated with the EAWM and its strength depends on the movement of the ITCZ (Yancheva et al., 2007). Average surface air temperature and precipitation, reconstructed across the East Asian monsoon region during the past 1000 years, document the strength of EASM during Little Ice age and Medieval Warm period (Zhou et al., 2011) (Fig. 6). According to Sone et al. (2013), the EAWM brings moisture and generates frequent snowfall or rainfall when it crosses the warm oceanic waters of the East Sea (Japan Sea). The stalagmite $\delta^{18}O$ record of Fufugaguchi Cave suggests that the EAWM has brought variable amounts

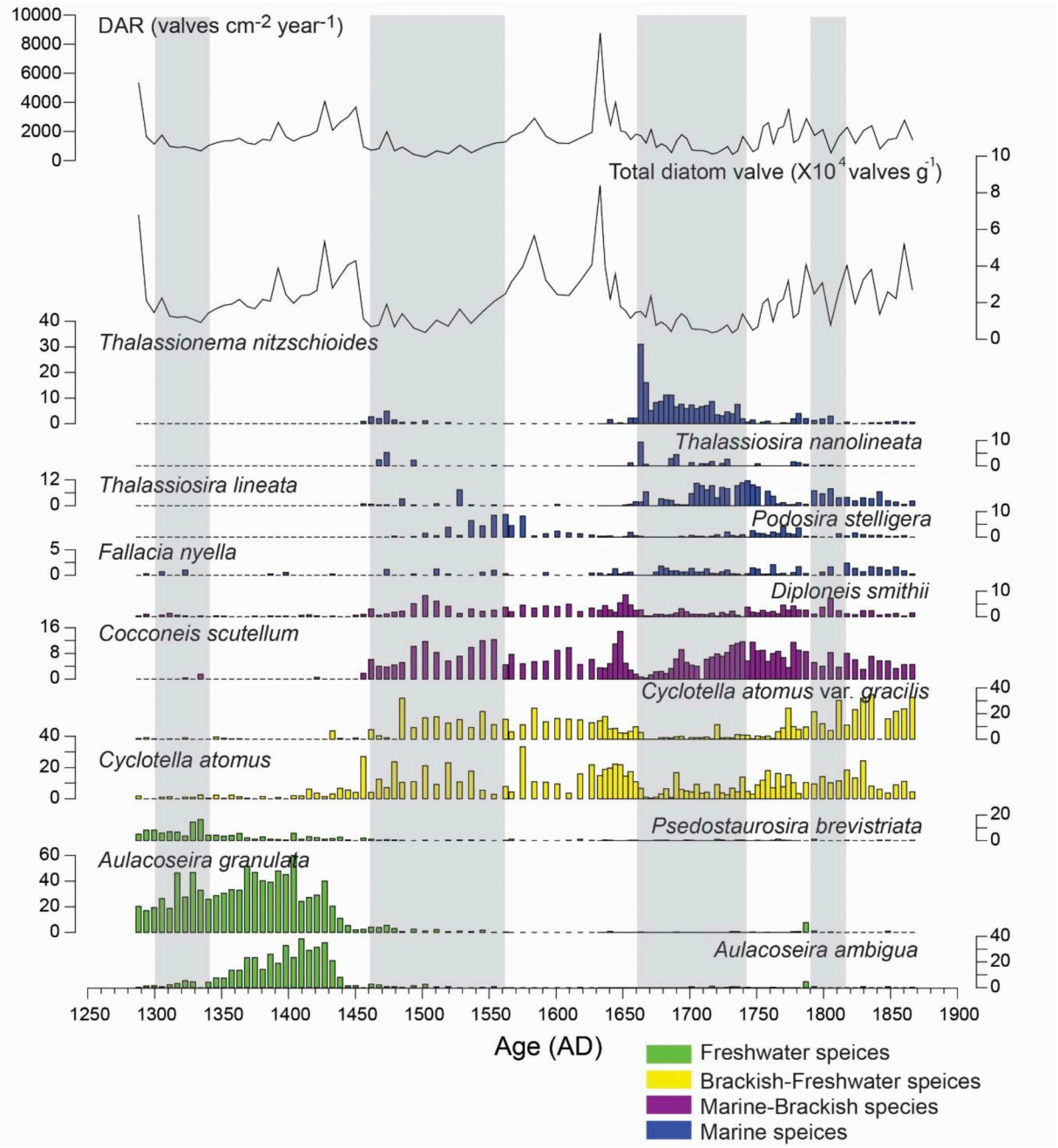

Fig. 5. Age distribution of diatom relative abundance by taxa, DAR and total diatom valves in core 16Hm-2C are categorized as freshwater, brackish-freshwater, marine-brackish, and marine species.

of moisture from the East Sea (Japan Sea) to western Japan over past 10,000 years (Fig. 6). In fact, for Itoigawa city, in northwest Japan, the average monthly precipitation was over 300 mm from November to January during the past ten years (Fig. 1). In contrast, the Pacific side of Japan is much drier, with average monthly rainfall less than 120 mm November to February and 50–70 mm from December to January during the past ten years in Hamamatsu city, Shizuoka Prefecture (Fig. 1). The impact of the EAWM is very different depending on location, with a strong contrast between northwest Japan and the Pacific side of Japan (Fig. 1).

The diatom abundance and composition are controlled by nutrients. The nutrient input and transfer to Lake Hamana will depend on rainfall (Anderson, 2000). A strong winter monsoon leads to low precipitation and cold temperatures on the Pacific side of Japan. On the other hand, the summer monsoon results in high precipitation and warm temperatures in Lake Hamana (Fig. 1). The salinity change in this lagoon has probably been dependant on precipitation. Although there is no record of centennial scale sea-level and tidal prism history in central Japan before the 19th century, sea-level was generally lower during the Little Ice Age (e.g., Akasofu, 2010). Contrary to what we would expect from a lower sea-level, marine taxa in Lake Hamana increased during the Little Ice Age (Fig. 5). This suggests that rainfall had a stronger impact on lake salinity than sea-level change. Therefore, it appears that indicators of primary production, such as TOC, diatom amounts (total diatom valve and DAR), and the composition of the diatom assemblage were strongly influenced by precipitation and its impact on nutrient input and lake salinity. Overall the precipitation amounts are tied to the competing strengths of the EASM and EAWM.

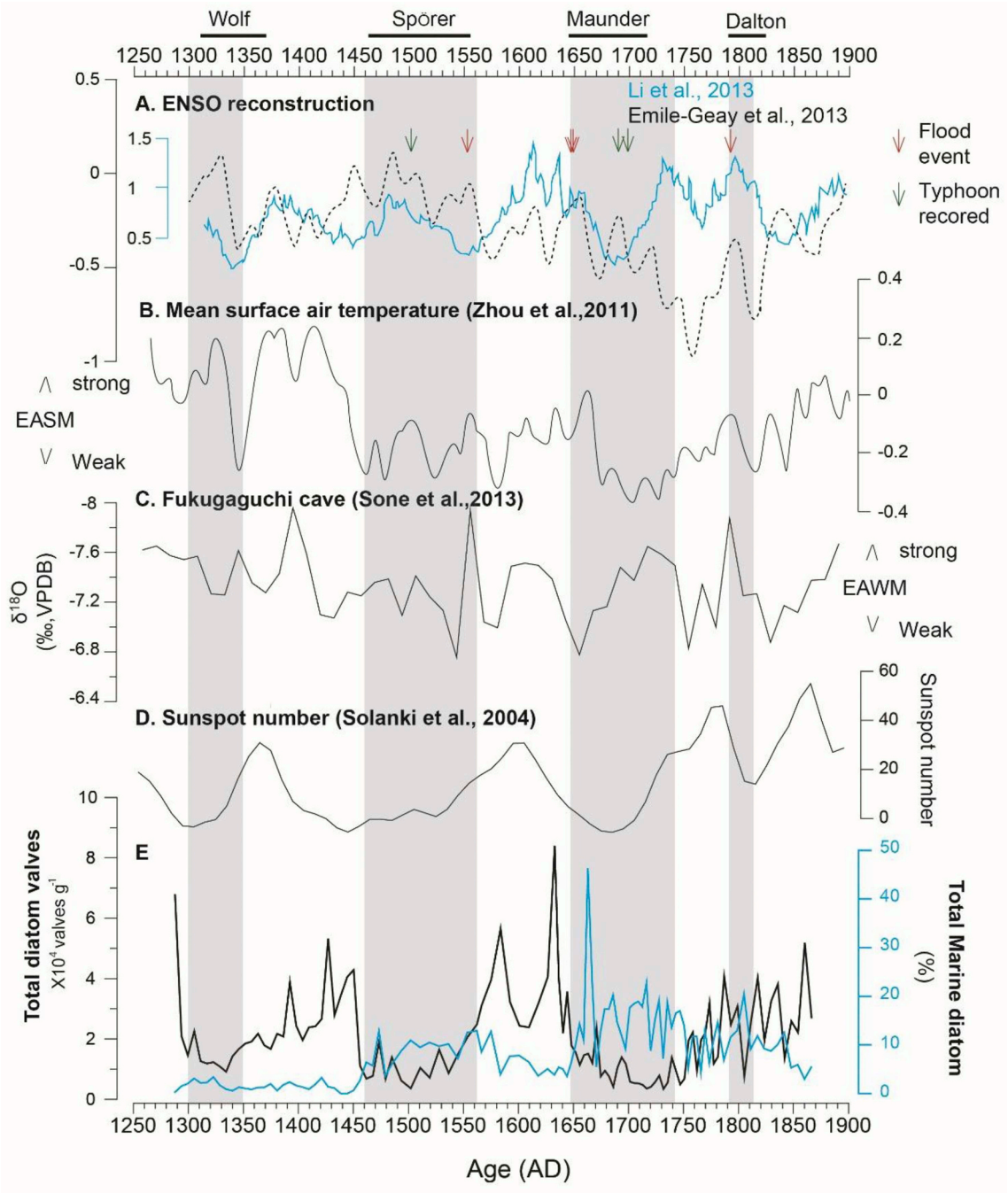

Fig. 6. Time comparisons: (A) ENSO reconstruction. Blue line is modified from Li et al. (2013). Dotted line is modified from Emile-Geay et al. (2013). (B) Mean surface air temperature over the East Asia monsoon region is modified from Zhou et al. (2011). (C) EAWM intensity of stalagmites from Fukugaguchi Cave (Sone et al., 2013). (D) Sunspot number based on dendrochronologically dated radiocarbon concentrations (Solanki et al., 2004). (E) Total diatoms and total marine diatoms in core 16Hm-2C. Wolf, Spörer, Maunder, and Dalton are regarded as a minimum solar event. (For interpretation of the references to color in this figure legend, the reader is referred to the Web version of this article.)

5.2.1. Relationship with EASM

In the 16Hm-2C core of Lake Hamana, the total number of diatom valves generally correlates with a strong EASM and an increased number of sunspots (Fig. 6). Additionally, sand and water content increased when the EASM and sunspot frequency intensified (Figs. 4 and 6). Sand at the core site was probably delivered by the river and with increased sand in the core the water content increases because porosity increases. *Cyclotella atomus* var. *gracilis* lives in euryhaline conditions, which is an indicator of a eutrophic setting (Genkal and Kiss, 1993). This taxon also appeared when the summer monsoon intensified after Lake Hamana became a brackish lagoon. These results suggest that diatom abundance increased in times of high solar activity and Lake Hamana became eutrophic. This is because a strong EASM triggers high precipitation for central Japan, and heavy precipitation drives terrestrial nutrients into the lake along with coarse sand. After 1750 CE, sand content did not increase to earlier levels because the seagrass *Zostera marina* interrupted input of sand. This *Z. marina* increased following the increase in solar activity after 1750 CE (Fig. 6.). When Lake Hamana was an oligohaline lake, *A. ambigua* and *A. granulata* were dominant, in the interval 1350–1440 CE (Fig. 5). High levels of these *Aulacoseira* taxa appeared during periods of a strong EASM. *Aulacoseira ambigua* and *A. granulata* usually inhabit mesotrophic and eutrophic environments

(Joh, 2010). Under oligohaline lake conditions, a strong EASM also produced significant diatom productivity and lake eutrophication.

5.2.2. Climate change during LIA

From 1645 CE–1740, the total number of diatom valves decreased and *T. nitzschioides*, which inhabits the neritic zone (Hallegraeff, 1986), became dominant, rising to 38% of the assemblage (Fig. 5). These results can be attributed to decreased precipitation and increased salinity. In addition, the C/N ratio shows the highest value during this period (Fig. 4). A high C/N ratio usually indicates an input of terrestrial material because the land plants contain high amounts of nitrogen-depleted lignin and cellulose unlike aquatic plankton (Lamb et al., 2006). The seagrass *Zostera marina* is distributed in the shallows and inlet of Lake Hamana (Sato et al., 2016). Seagrasses also have a high C/N ratio, and it is common to see the reefs of *Z. marina* in Lake Hamana. This seagrass is transported into the lake by the tides at present. Therefore, a high C/N ratio may be explained by significant sea-water inflow. In the lagoon, the salinity is primarily controlled by rainfall because sea level has been mostly stable for the last 1000 years (Umitsu, 1991). During 1460–1560 CE, total marine taxa increased to greater than 10% and *T. nitzschioides* also showed an increase (Figs. 5 and 6). Between 1790 CE and 1810, the total number of diatom valves decreased and marine diatoms suddenly increased. Total diatom valve number and marine taxa abundance showed similar patterns during 1460–1560 CE and 1790–1810 CE (Figs. 5 and 6). On the other hand, when Lake Hamana was an oligohaline lake, an increase of marine taxa did not occur. However, a dramatic change of dominant taxa still happened. *Aulacoseira ambigua* suddenly dropped to low abundances, while *P. brevistriata* increased. These changes happened against the backdrop of a decrease in the total number of diatom valves during 1300–1350 CE (Figs. 5 and 6). *Aulacoseira ambigua* prefers high temperatures and high light intensities compared to other species (Shear et al., 1976). *Pseudostaurosira brevistriata* is a benthic freshwater species and inhabits oligotrophic lakes (Joh et al., 2010). Low precipitation in the catchment must have resulted in lower sediment and nutrient input. Therefore, *P. brevistriata* increased during 1300–1350 CE when sunlight reached the bottom of the lake, indicative of a change to an oligotrophic lake. However, in the early LIA, 1320 CE–1350, the EASM increased, and EAWM decreased, in a trend counter to solar irradiance changes (Fig. 6). Total diatom numbers were still low even though there was a small increase at the beginning of 14th century (Fig. 6). The reason why might be a reduction in solar irradiance and its impact on photosynthesis. Also, TOC decreased during these periods (1300–1350 CE, 1460–1560, 1645–1740 and 1790–1810), well synchronized with low counts of total number of diatom valves (Figs. 4 and 5). The small change of TOC from 1300 CE–1350 is because Lake Hamana was an oligohaline lake at that time. The EASM and sunspot number show a trend very similar to diatom and chemical data. Therefore, these periods (1300–1350 CE, 1460–1560, 1645–1740 and 1790–1810) fall within the climate interval defined as the LIA (Fig. 6). These diatom results suggest that the amount of precipitation decreased during the LIA due to the weak monsoon in these periods.

In contrast, before 1650 CE the EAWM is not in a strongly anti-correlated relationship with the EASM and sun spot record, based on our data (Fig. 6). One of the most likely reasons for this is because of the low resolution of the long stalagmite record, which is used as the basis of the EAWM proxy that covers the last 10,000 years. In it the last 500 years is represented by less than 50 data points (Sone et al., 2013). In addition, the EAWM climate of the Sea of Japan side and the Pacific side of Japan is very different today and is likely to have been different in the past.

5.3. Flood events related to ENSO during the Little Ice Age

In the Asian monsoon area, significant amounts of extreme precipitation are induced by typhoons (Fumin et al., 2002; Kim et al., 2006; Ge et al., 2010; Lee et al., 2010). This typhoon pattern is strongly affected by ENSO, and typhoons tend to recurve to Japan, South Korea, and Northern China during El Niño events (Elsner and Liu, 2003). The typhoons occur from July to October and lead to very heavy rainfall when they occur in September and October (Fig. 1). However, when typhoons do not occur during the fall season the monthly precipitation tends to be low (Fig. 1).

Evidence for typhoons, for example sand deposits, were found as overwash deposits from the Lake Hamana barrier beach (Komatsubara et al., 2008). Woodruff et al. (2009) used strontium (Sr), which was derived from a lagoon barrier beach to identify storm deposits. However, there are no sand deposits in the 16Hm-2C core because the coring site is too far away from the sandbar and inflowing streams. Based on tide direction, the sediments are transported from the Miyakoda River to the coring site (Fig. 1.) (Taguchi and Nakata, 1998). In addition, the seagrass *Zostera marina* is distributed in shallow parts of Lake Hamana (Sato et al., 2016). Therefore, sand, which is transported as bed load, is blocked by *Zostera marina* beds.

High-density layers in the soft X-ray images were present at 1550 CE, 1645, 1650, and 1790 (Fig. 3). These layers are well correlated with peaks of *Achanathidium minutissimum* (Fig. 3). *Achanathidium minutissimum* is a benthic freshwater species (Joh, 2012), and can be an indicator of terrestrial input accompanied by inflow of river water in the lagoon. In addition, magnetic susceptibility is controlled by pedogenesis and deposition of dust that are both dependent on precipitation (An et al., 1991). Magnetic susceptibility also increased during those periods (Fig. 3). Ample rainfall might have induced flooding that resulted in the deposition of *A. minutissimum*, which inhabits only freshwater environments such as streams or lakes. Therefore, these high-density layers are used as proxies of flood layers, which might be deposited after heavy rain events in the Lake Hamana catchment. Several typhoon events in Shizuoka Prefecture have been recorded in historical documents. A storm which occurred in 1509 CE destroyed the bridge at the mouth of Lake Hamana. Other storms in 1680 CE and 1699 washed away houses in Shizuoka Prefecture (Komatsubara et al., 2008).

The possibility that one of these flooding event layers was caused by the tsunami associated with the Meio earthquake is very low. These flood events are more likely associated with high amounts of precipitation induced by the intensity of EASM and typhoons accompanied by heavy rainfall. It is hard to distinguish these event layers whether typhoon or tsunami deposit based on lithological condition because these layers are so thin. An important feature that argues against a tsunami deposit is that there was no marine diatom in these layers, although the marine diatoms are common in tsunami deposits because the tsunami brings offshore marine water and sediment far inland. For example, a large amount of marine diatoms were deposited in the tsunami deposit generated by the 2004 Indian Ocean tsunami at Phra Thong Island, Thailand (Sawai et al., 2009). Furthermore, these event layers are not synchronous with the Meio earthquake, which occurred in 1498 CE. These layers, therefore, were probably not formed by tsunami events. The diatom assemblages and lithology suggest these flood sediments were deposited when the EASM was weak, not strong. This suggests that these flood event layers were not formed by a high amount of precipitation under an intensified EASM. Therefore, the event layers are most strongly related to typhoons accompanied by very heavy rainfall.

An ENSO record has been reconstructed based on 2222 tree-ring chronologies and by modeling over the past several centuries (Emile-Geay et al., 2013; Li et al., 2013) (Fig. 6). Red arrows, marking flood events in Lake Hamana, and green arrows indicating typhoon events from historical records synchronize with some of the peaks in of the ENSO record in Fig. 6. Some events, however, do not clearly match with both reconstructed ENSO peaks, perhaps due to disagreements in the different reconstructed ENSO records (Fig. 6). Including events from the historical record and our record of flood deposits (1550 CE, 1645, 1650, and 1790) flood frequency increased during the LIA (Fig. 6). Another

study makes the same observation; typhoon frequency increased during LIA in Hwajinpo lagoon, Korea (Katsuki et al., 2016). As mentioned above, the EASM was weak during the LIA, and the amount of precipitation was lower than in other periods. ENSO is strongly related to sea surface temperature (SST) in the Pacific Ocean (Schwing et al., 2002; Marchitto et al., 2010). This SST is also affected by solar activity. Marchitto et al. (2010) showed that proxy-based SST records based on Mg/Ca ratio correlated with the generation of cosmogenic nuclides ^{14}C and ^{10}Be. Therefore low solar activity is correlated with El Niño-like conditions (Marchitto et al., 2010). Japan has a complicated climate system, but it is one that is closely related to solar insolation. The climate of Japan over the last 1000 years has undergone significant variation. The LIA was in place for about 650 years from 1300–1950 CE (Matthews and Briffa, 2005). Before the LIA, the Medieval Solar Maximum occurred from 1100 CE–1250 (Jirikowic and Damon, 1994). During the LIA, El Niño was strong, and typhoons during El Niño years tended to recurve to the northeast (Wang and Chan, 2002), which may increase the likelihood of typhoons making landfall in Japan (Elsner and Liu, 2003). The heavy precipitation levels induced by typhoons in Japan is strongly dependent on the typhoon strength and the study area's distance from the typhoon. Therefore, even if many typhoons make landfall in central Japan, they do not always result in heavy rains on Lake Hamana. On the other hand, strong storms around Lake Hamana in historical documents, and flood records in core 16Hm-2C, represented by flood layer deposits and peaks in *A. minutissimum* abundance, can be matched to strong ENSO events during the LIA (Figs. 1 and 6). We suggest that a strong El Niño during the LIA might lead to frequent typhoon events in Japan, accompanied by significant floods.

6. Conclusion

This research documented paleoenvironmental and climate changes in eastern central Japan during the LIA by analysis of diatom assemblages and chemical components of an AMS ^{14}C dated core of lake sediments. Lake Hamana changed from an oligohaline lake to a brackish lagoon in the mid-15th century because of changes in the flow volume of the Hamana paleoriver. This occurred before the Meio earthquake. The diatom assemblage in Lake Hamana shows a strong relationship to the strength of the EASM. When the EASM intensified, diatom abundance increased due to high rainfall and river runoff and Lake Hamana became eutrophic. Diatom productivity decreased under increasing sea water inflow when the EASM weakened during the LIA. Lake Hamana was often affected by flooding events induced by typhoons based on historical data and flood deposits in the core. During the LIA, frequent typhoons impacted central Japan because typhoons move toward Japan under El Niño-like conditions.

Acknowledgments

Financial support from the JSPS KAKENNHI Grant (No. 17K18537 & 17H02974), Japan and Research Grant of the Museum of Natural and Environmental History, Shizuoka, Japan (2016–2017) (reference to Prof. Yamada) are gratefully acknowledged. We appreciate Dr. David L. Dettman of Arizona University revise the English grammar.

References

Akasofu, S., 2010. On the recovery from the Little Ice age. Nat. Sci. 2, 1211–1224.
An, Z., Kukla, G.J., Porter, S.C., Xiao, J., 1991. Magnetic susceptibility evidence of monsoon variation on the Loess Plateau of central China during the last 130,000 years. Quat. Res. 36, 29–36.
Anderson, N.J., 2000. Miniview: diatoms, temperature and climatic change. Eur. J. Phycol. 35, 307–314.
Berner, R., Raiswell, R., 1984. C/S method for distinguishing freshwater from marine sedimentary rocks. Geology 12, 365–368.
Ebara, M., 2008. Travels along the Medieval Tokaido (Chuseino Tokaido Wo Yuku). Chuokoron-shinsha, Tokyo (in Japanese).
Elsner, J.B., Liu, K.B., 2003. Examining the ENSO-typhoon hypothesis. Clim. Res. 25, 43–54.
Emile-Geay, J., Cobb, K.m., Mann, M.E., Wittenberg, A.T., 2013. Estimating central equatorial pacific SST variability over past millennium. Part I: methodology and validation. J. Clim. 26, 2302–2328.
Fujiwara, O., Komatsubara, J., Takada, K., Shishikura, M., Kamataki, T., 2006. Temporal development of a late Holocene strand plain system in the Shirasuka area along western Shizuoka prefecture on the pacific coast of Central Japan. J. Geogr. 115, 569–581 (in Japanese with English abstract).
Fujiwara, O., Ono, E., Yata, T., Umitsu, M., Sato, Y., Heyvaert, V.M.A., 2013. Assessing the impact of 1498 Meio earthquake and tsunami along the Enshu-nada coast, central Japan using coastal geology. Quat. Int. 308–309, 4–12.
Fumin, R., Gleason, B., Easterling, D., 2002. Typhoon impacts on China's precipitation during 1957-1996. Adv. Atmos. Sci. 19, 943–952.
Ge, X., Li, T., Zhang, S., Peng, M., 2010. What causes the extremely heavy rainfall in Taiwan during Typhoon Morakot (2009)? Atmos. Sci. Lett. 11, 46–50.
Genkal, S.I., Kiss, K.T., 1993. Morphological variability of the diatom *Cyclotella atomus* Hustedt var. *atomus* and *C. atomus* var. *gracilis* var. nov. Hydrobiologia 269–270, 39–47.
Gupta, A.K., Anderson, D.M., Overpeck, J.T., 2003. Abrupt changes in the Asian southwest monsoon during the Holocene and their links to the north Atlantic ocean. Nature 421, 354–357.
Hallegraeff, G.M., 1986. Taxonomy and morphology of the marine plankton diatoms Thalassionema and Thalassiothrix. Diatom Res. 1, 57–80.
Hasle, G.R., Syvertsen, E.E., 1996. Marine diatoms. In: Tomas, C.R. (Ed.), Identifying Marine Phytoplankton. Academic Press, San Diego, pp. 5–386.
Hendey, N.I., 1964. An introductory account of the smaller algae of British coastal water, part V : Bacillariophyceae (Diatoms). Otto Koeltz Science, Koenigstein.
Isomi, H., Inoue, M., 1972. Geology of the Hamamatsu District - Quadrangle Series Scale 1:50,000 Kyoto (11) No. 59. Geological Survey of Japan, Kawasaki (in Japanese).
Japan Meteorological Agency, 2018. (in Japanese). http://www.data.jma.go.jp/gmd/risk/obsdl/index.php.
Japan Meteorological Agency, 2017. (in Japanese). https://www.data.jma.go.jp/gmd/kaiyou/db/tide/gaikyo/nenindex.php.
Jirikowic, J.L., Damon, P.E., 1994. The Medieval solar activity maximum. The Medieval Warm Period. Springer, Dordrecht, pp. 309–316.
Joh, G.J., 2010. Algal Flora of Korea Volume3 Number1 Freshwater Diatoms I. National Institute of Biological Resource, Incheon, pp. 152.
Joh, G.J., 2012. Algal Flora of Korea Volume3 Number7 Freshwater Diatoms V. National Institute of Biological Resource, Incheon, pp. 132.
Joh, G.J., Lee, J.H., Lee, K.,, Yoon, S.K., 2010. Algal Flora of Korea Volume3 Number2 Freshwater Diatoms II. National Institute of Biological Resource, Incheon, pp. 153.
Kashima, K., 1985. Holocene diatom assemblages in Takagami Lowland, central part of Choshi Peninsula, and its relation to changes of sea-level. Quat. Res. 24, 125–138.
Kashima, K., 1986. Holocene successions of diatom fossil assemblages in alluvium, and those relations to paleo-geographical changes. Geogr. Rev. Jpn. 59, 383–403.
Kashima, K., 1988. Paleo-environmental succession in Lake Hamana presumed by diatom analysis. Clastic sediments 5, 95–107.
Katsuki, K., Yang, D.Y., Seto, K., Yasuhara, M., Takata, H., Otsuka, M., Nakanishi, T., Yoon, Y., Um, I.K., Cheung, R.C.W., Khim, B.K., Kashima, K., 2016. Factors controlling typhoons and storm rain on the Korean Peninsula during the Little Ice age. J. Paleolimnol. 55, 35–48.
Katsuki, K., Yang, D.Y., Lim, J., Lee, J.Y., Asahi, H., Han, M., 2017. Multi-centennial-scale changes in East Asian typhoon frequency during the mid-Holocene. Palaeogeogr. Palaeoclimatol. Palaeoecol. 476, 140–146.
Kim, J., Ho, C., Lee, M., Jeong, J., Chen, D., 2006. Large increase in heavy rainfall associated with tropical cyclone landfalls in Korea after the late 1970s. Geophys. Res. Lett. 33, L18706.
Kobayashi, H., Idei, H., Mayama, S., Nagumo, T., Osada, K., 2006. H. Kobayasi's Atlas of Japanese Diatoms Based on Electron Microscopy ume 1 Uchida Rokakuho Publishing, Tokyo (in Japanese).
Kojima, S., Suto, R., Chihara, M., 1995. Catalogue of Environmental Microorganisms. Kodansha Publishing, Tokyo (in Japanese).
Komatsubara, J., Fujiwara, O., Takada, K., Sawai, Y., Aung, T.T., Kamataki, T., 2008. Historical tsunamis and storms recorded in a coastal lowland, Shizuoka Prefecture, along the Pacific Coast of Japan. Sedimentology 55, 1703–1716.
Lamb, A.L., Wilson, G.P., Leng, M.J., 2006. A review of coastal palaeoclimate and relative sea-level reconstructions using δ13C and C/N ratios in organic material. Earth Sci. Rev. 75, 29–57.
Lee, M.-H., Ho, C.-H., Kim, J.-H., 2010. Influence of tropical cyclone landfalls on spatiotemporal variations in typhoon season rainfall over South China. Adv. Atmos. Sci. 27, 443–454.
Li, J., Xie, S.P., Cook, E.R., Morales, M.S., Christie, D.A., Johnson, N.C., Chen, F., D'Arrigo, R., Fowler, A.M., Gou, X., Fang, K., 2013. El Niño modulations over the past seven centuries. Nat. Clim. Change 3, 822–826.
Linick, T.W., Damon, P.E., Donahue, D.J., Jull, A.J.T., 1989. Accelerator mass spectrometry: the new revolution in radiocarbon dating. Quat. Int. 1, 1–6.
Matthews, J.A., Briffa, K.R., 2005. The "Little Ice Age": re-evaluation of an evolving concept. Geogr. Ann. Ser. A Phys. Geogr. 17–36.
Marchitto, T.M., Muscheler, R., Ortiz, J.D., Carriquiry, J.D., Geen, A. Van, 2010. Dynamical response of the tropical Pacific Ocean to solar forcing during the early Holocene. Science 330, 1378–1381.
Matsubara, A., 2001. Coastal barriers in Hamana lake and the Hamamatsu lowland. In: The Hiyoshi Review of Social Sciences. vol. 11. Keio University, pp. 20–32 (in Japanese).
Matsubara, A., 2007. Relationships between geomorphic development of coastal ridges and human activities: a case study of the Hamamatsu and Haibara lowlands. In: The

Hiyoshi Review of Social Sciences. vol. 18. Keio University, pp. 1–13 (in Japanese).
Morita, H., Kashima, K., Takayasu, K., 1998. Paleoenvironmental changes of Lake Hamana and Lake Shinji during the last 10,000 years, inferred by diatom assemblages from lake core sediments. Laguna 5, 47–53.
Muto, T., 1987. Geology of the Mikatagahara and Iwatabara Terraces, in the lower Tenryugawa River area, Japan—an interpretation from the present dissected alluvial fan. J. Geol. Soc. Japan 93, 259–273.
Nakashima, R., Mizuno, K., Furusawa, A., 2008. Depositional age of the middle Pleistocene Atsumi group in Atsumi Peninsula, central Japan, based on tephra correlation. J. Geol. Soc. Japan 114, 70–79 (in Japanese with English abstract).
Park, J.S., Jung, S.W., Lee, S.D., Yun, S.M., Lee, J.H., 2016. Species diversity of the genus *Thalassiosira* (Thalassiosirales, Bacillariophyta) in South Korea and its biogeographical distribution in the world. Phycologia 55 (4), 403–423.
Peros, M., Gregory, B., Matos, F., Reinhardt, E., Desloges, J., 2015. Late-Holocene record of lagoon evolution, climate change, and hurricane activity from southeastern Cuba. Holocene 25, 1483–1497.
Reimer, P.J., Bard, E., Bayliss, A., Beck, J.W., Blackwell, P.G., Ramsey, C.B., Buck, C.E., Cheng, H., Edwards, R.L., Friedrich, M., 2013. IntCal13 and Marine13 radiocarbon age calibration curves 0–50,000 years cal BP. Radiocarbon 55, 1869–1887.
Round, F.E., Craword, R.W., Mann, D.G., 1990. The Diatoms: Biology and Morphology of the Genera. Cambridge University Press, Cambridge.
Ryu, E., Ryu, B.J., Yun, H., Lee, S.J., 2003. Diatom floras of the Ulleung basin: implication for late quaternary paleoenvironment. J. Geol. Soc. Korea 39, 183–198.
Sato, M., Horinouchi, M., Fujita, M., Sano, M., 2016. Responses of fish assemblage structures to annual and perennial life cycles of seagrass Zostera marina in Lake Hamana, central Japan. Ichthyol. Res. 63, 445–459.
Sato, Y., Matsuoka, H., Okamura, M., Kashima, K., 2016. Late Holocene environmental changes of coastal lagoon inferred from a fossil diatom analysis of sediment core from Lake Hamana, central Japan. Quat. Int. 397, 317–329.
Sawai, Y., Jankaew, K., Martin, M.E., Prendergast, A., Choowong, M., Charoentitirat, T., 2009. Diatom assemblages in tsunami deposits associated with the 2004 Indian Ocean tsunami at Phra Thong Island, Thailand. Mar. Micropaleontol. 73, 70–79.
Schwing, F.B., Murphree, T., deWitt, L., Green, P.M., 2002. The evolution of oceanic and atmospheric anomalies in the northeas Pacific during the El Niño and la Niña events of 1995-2001. Prog. Oceanogr. 54, 459–491.
Shear, H., Nalewajko, C.N., Bacchus, H.M., 1976. Some aspects of the ecology of Melosira spp. in Ontario Lakes. Hydrobiologia 50, 173–176.
Shishikura, M., Echigo, T., Kaneda, H., 2007. Marine reservoir correction for the Pacific coast of central Japan using ^{14}C ages of marine mollusks uplifted during historical earthquakes. Quat. Res. 67, 286–291.
Solanki, S.K., Usoskin, I.G., Kromer, B., Schüssler, M., Beer, J., 2004. Unusual activity of the Sun during recent decades compared to the previous 11,000 years. Nature 431, 1084–1087.
Sone, T., Kano, A., Okumura, T., Kashiwagi, K., Hori, M., Jiang, X., Shen, C.C., 2013. Holocene stalagmite oxygen isotopic record from the Japan Sea side of the Japanese Islands, as a new proxy of the East Asian winter monsoon. Quat. Sci. Rev. 75, 150–160.
Stuiver, M., Reimer, P.J., 1993. Extended 14 C data base and revised CALIB 3.0 14C age calibration program. Radiocarbon 35, 215–230.
Sugiyama, Y., 1991. The Middle Pleistocene deposits in the Atsumi Peninsula and along the east coast of Lake Hamana, Tokai district-sedimentary cycles formed by the glacio-eustatic sea-level change and their correlations to the contemporaneous deposits in the Kanto and Kinki. Bull. Geol. Surv. Jpn. 42, 75–109 (in Japanese with English abstract).
Taguchi, K., Nakata, K., 1998. Analysis of water quality in Lake Hamana using a coupled physical and biochemical model. J. Mar. Syst. 16, 107–132.
Takano, H., 1990. Diatoms. In: Fukuyo, Y., Takano, H., Chihara, M., Matsuoka, K. (Eds.), Red Tide Organisms in Japan: an Illustrated Taxonomic Guide. Uchida Rokakuho, Tokyo, pp. 162–331.
Umitsu, M., 1991. Holocene sea-level changes and coastal evolution in Japan. Quat. Res. 30, 187–196.
Wang, B., Chan, J.C.L., 2002. How strong ENSO events affect tropical storm activity over the western North Pacific. J. Clim. 15, 1643–1658.
Wang, Y., Cheng, H., Edwards, R.L., He, Y., Kong, X., An, Z., Wu, J., Kelly, M.J., Dykoski, C.A., Li, X., 2005. The Holocene Asian monsoon: links to solar changes and North Atlantic climate. Science 308, 854–857.
Watanabe, H., 1998. Comprehensive List of Tsunamis Hit the Japanese Islands, second ed. University of Tokyo Press, Tokyo (in Japanese).
Watanabe, T., 2005. Picture Book and Ecology of the Freshwater Diatoms. Uchida Rokakuho Publishing, Tokyo (in Japanese).
Witkowski, A., Lange-Bertalot, H., Metzeltin, D., 2000. Diatom Flora of Marine Coasts I. In: Gantner, A.R.G., Verlag, K.G., Ruggell (Eds.), Iconographia Diatomologica. vol. 7. pp. 925.
Woodruff, J.D., Donnelly, J.P., Okusu, A., 2009. Exploring typhoon variability over the mid-to-late Holocene: evidence of extreme coastal flooding from Kamikoshiki, Japan. Quat. Sci. Rev. 28, 1774–1785.
Woodruff, J.D., Kanamaru, K., Kundu, S., Cook, T.L., 2015. Depositional evidence for the Kamikaze typhoons and links to changes in typhoon climatology. Geology 43, 91–94.
Woodward, C., Shulmeister, J., Bell, D., Haworth, R., Jacobsen, G., Zawadzki, A., 2014. A Holocene record of climate and hydrological changes from Little Llangothlin Lagoon, south eastern Australia. Holocene 24, 1665–1674.
Yancheva, G., Nowaczyk, N.R., Mingram, J., Dulski, P., Schettler, G., Negendank, J.F.W., Liu, J., Sigman, D.M., Peterson, L.C., Haug, G.H., 2007. Influence of the intertropical convergence zone on the East Asian monsoon. Nature 445, 74–77.
Yata, T., 2005. The damages by tsunami in Meiou-Toukai earthquake in 1498 and the suffering in Anotsu in the Middle Ages. Hist. Earthquakes (Rekishi Jisin) 20, 9–12 (in Japanese).
Yata, T., 2009. Large Earthquakes Occurred in Medieval Period Recorded in Japanese History. Yoshikawa-kobunkan, Tokyo (in Japanese).
Yoneda, M., Uno, H., Shibata, Y., Suzuki, R., Kumamoto, Y., Yoshida, K., Sasaki, T., Suzuki, A., Kawahata, H., 2007. Radiocarbon marine reservoir ages in the western Pacific estimated by pre-bomb molluscan shells. Nucl. Instrum. Methods Phys. Res. B. 259, 432–437.
Zhou, X.J., Zhao, P., Liu, G., Zhou, T.J., 2011. Characteristics of decadal-centennial-scale changes in east Asian summer monsoon circulation and precipitation during the medieval Warm period and Little Ice age and in the present day. Chin. Sci. Bull. 56, 3003–3011.